Aeolian Research 51 (2021) 100712

Contents lists available at ScienceDirect

Aeolian Research

journal homepage: www.elsevier.com/locate/aeolia

# Aeolian sand transport over a wet, sandy beach

C. Swann [a,*], D. Lee [a,b], S. Trimble [a,b], C. Key [a]

[a] U.S. Naval Research Laboratory, Sediment Dynamics Section, Ocean Sciences Division, Stennis Space Center, MS, United States
[b] National Research Council Research Associateship Program, National Academy of Sciences, Washington D.C., United States

ARTICLE INFO

*Keywords:*
Aeolian transport
Vertical flux profiles
Moisture content
Saltation
Windblown sand
Transport dynamics

ABSTRACT

Quantifying aeolian transport within the intertidal zone is critical to understanding feedbacks between aeolian and nearshore processes in coastal environments. Here, we report a field study of aeolian transport over a wet bed in the intertidal zone. Predominate winds and beach orientation were aligned during all field observations. Mean grain size of bed samples were 0.18 mm and moisture content ranged from 16 to 17%. Velocity profiles were measured with a vertical array of cup anemometers. Sustained wind velocities were 9.5 m/s at 93 cm above the bed with gusts reaching 13.5 m/s. Five saltation traps captured particles in transport from the bed to a height of 15 cm. Particles in transport were wet and the highest moisture content of trapped sediments was found in the lowest saltation trap. Vertical flux profiles show a higher concentration of flux closer to the bed (81 to 89% below 5 cm) than those measured over dry beds. Power and exponential decay functions were fit to our vertical flux profiles; the exponential decay function best fit flux profiles with larger $\beta$ coefficients and smaller $\alpha$ estimates than those fit to dry bed profiles. Total flux models predict transport below Belly's (1964) fluid threshold of motion for moist beds and model performance improves when using a threshold for dry sand. Our results suggest transport over wet beds is fundamentally different from transport over dry beds. However, more research is needed to discern the mechanics driving deviations in flux profiles over wet beds in field environments.

## Introduction

Quantifying aeolian transport on the subaerial beach is critical to understanding feedbacks between aeolian and nearshore processes in coastal environments. Cross-shore moisture gradients from the more wet, intertidal zone to the drier, upper beach are an important control on aeolian transport (Namikas and Sherman, 1995; Davidson-Arnott and Bauer, 2009; Delgado-Fernandez and Davidson-Arnott, 2011; de Vries et al., 2014). The most commonly used transport models predicting total transport flux across these gradients of moisture (Bagnold, 1936; Kawamura, 1951; Chepil, 1945; Zingg, 1953; Lettau and Lettau, 1978) are derived in wind tunnels with idealized surface conditions (cohesionless, dry beds comprised of uniform grain size distributions), and simply use a threshold term to account for changes in moisture content (Belly, 1964). However, these models perform poorly when tested in field environments (Davidson-Arnott and Bauer, 2009; de Vries et al., 2014; Delgado-Fernandez and Davidson-Arnott, 2011; Horikawa et al., 1986; Nield and Wiggs, 2011; Rotnicka, 2013; Sherman et al., 1998, 2013; Wiggs et al., 2004; Davidson-Arnott et al., 2005) and often yield contradictory results. For example, the presence of moisture has been documented to reduce (Davidson-Arnott and Bauer, 2009; Delgado-Fernandez and Davidson-Arnott, 2011; Han et al., 2012), increase (Rotnicka, 2013), and have minimal impact on total transport flux (Kawata, 1950; Hotta et al., 1984; McKenna-Neuman and Scott, 1998; Wiggs et al., 2004). Decreases or minimal differences in transport flux are largely attributed to (1) limited sediment availability due to the fluid threshold required to initiate motion on a wet bed being higher than the shear stress imparted on the bed (Wiggs et al., 2004; Delgado-Fernandez and Davidson-Arnott, 2011; de Vries et al., 2014), or (2) transport intermittency where repeated drying and stripping of thin surface layers of upwind sediments leads to discontinuous transport (Cornelis and Gabriels, 2003; Wiggs et al., 2004; Davidson-Arnott and Bauer, 2009). Conversely, the field experiments of Rotnicka (2013) show total transport flux was up to 90% greater over a flat, moist bed than flux measured over a dry, rippled bed.

To resolve these discrepancies in total flux observations, wind tunnel studies have investigated the vertical distribution of flux to tease out the transport mechanics operating over wet beds (van Dijk and Stroosnijder, 1996; McKenna-Neuman and Scott, 1998; Han et al., 2012). In these controlled environments, particle speeds, trajectories, and impact and

* Corresponding author.
*E-mail address:* christy.swann@nrlssc.navy.mil (C. Swann).

https://doi.org/10.1016/j.aeolia.2021.100712
Received 14 August 2020; Received in revised form 26 April 2021; Accepted 3 May 2021
Available online 27 May 2021

ejection velocities (van Dijk and Stroosnijder, 1996; McKenna-Neuman and Scott, 1998; Han et al., 2012) can be measured to examine the coefficient of restitution, $e = \frac{v_r}{v_i}$, where $v_r$ and $v_i$ are the rebound and impact velocities, governing the height and ejection of transported particles. These studies often find an increase in salton velocity due to a higher $e$ causing particles to retain more of their energy upon collision with a hard, wet surface (McKenna-Neuman and Scott, 1998; Han et al., 2012; Comola et al., 2019; van Rijn and Strypsteen, 2020). However, even with the collision of high-energy saltons, the number of ejected particles can decrease due to moisture-induced interparticle cohesion between particles at rest (McKenna-Neuman and Scott, 1998; Comola et al., 2019). In these cases, wet beds act as transport pathways for saltating grains and there is minimal impact on transport flux as increased salton velocities are counterbalanced by a reduced number of ejecta (reptons or creep) due to cohesion. These effects should result in a larger number of saltating grains transported higher above the bed and a reduced number of particles close to the surface for transport over wet beds. However, these dynamics are not consistently observed in field environments. For example, field observations of vertical flux profiles over wet beds find higher concentrations of particles close to the surface (Rotnicka, 2013), suggesting the overall population of transported particles do not rebound as high over wet beds.

The discrepancy between wind tunnel and field observations makes it difficult to interpret the effects of moisture content on aeolian sand transport. Three fundamental grain scale mechanisms can alter total flux and vertical flux profiles over a wet bed: (1) particle collision on wet beds whose elasticities differ from dry beds and subsequently alters the coefficient of restitution, particle impact and ejection velocities, and the height of transported particles (van Dijk and Stroosnijder, 1996; McKenna-Neuman and Scott, 1998; Comola et al., 2019), (2) water wedges that form cohesive contact points between grains that require more energy to eject particles at rest (Belly, 1964; Namikas and Sherman, 1995), and (3) lubrication effects from the absorption of water on the surface of particles that can alter particle trajectories and particle-to-particle collisions (Barnocky and Davis, 1989; Pitois et al., 2000; Davis et al., 2002).

To date, there is no unifying theory to reconcile the observed discrepancies in aeolian transport over wet beds, making it difficult to adequately predict transport in field environments. In this paper, we use field observations of total transport flux and the distribution of flux with height to investigate the behavior of aeolian transport over a wet bed (w % = 16) in a natural environment.

## Study site and methods

### *Field site*

The field experiment was conducted as part of DUNEX (During Nearshore Event Experiment), an interagency collaborative experiment funded by the U.S. Coastal Research Program aimed at quantifying storm impacts along the Outer Banks of North Carolina. Field experiments were carried out on a fine-grained, dissipative beach about 6 km north of the municipality of Corolla, North Carolina, USA (Fig. 1). The study site is located along the coastal extent of the Currituck National Wildlife Refuge where foredune height varies between 6 and 8 m above NAVD88 mean sea level. The mean tidal range is 1.1 m. The subaerial beach width is 30–40 m and extends an additional 40 – 50 m during low tide. Beach sand is predominantly fine quartz with a mean diameter of 0.18 mm. The water line from wave runup was within 1–5 m of the instrument array during data collection (Fig. 2).

### *Experimental design*

Field observations were collected on a falling tide in the early morning hours of October 21, 2019 (Fig. 1). The intertidal zone was approximately 20 m wide and our instrument array was deployed on the recently exposed, flat intertidal zone (Figs. 1 and 2). Velocity profiles were measured using a vertical array of R.M. Young cup anemometers (Model 12102) at 0.07, 0.18, 0.44, 0.68 and 0.93 m above the surface and sampled at 32 Hz. Wind direction was measured at 2.0 m via an R.M. Young wind vane (Model 12302) and recorded at 1 Hz. Voltage outputs from the anemometers and the wind vane were hardwired to a National Instruments data acquisition system. Instrumentation heights were measured before and after the experiment to determine erosion or accretion of the surface during the observational period.

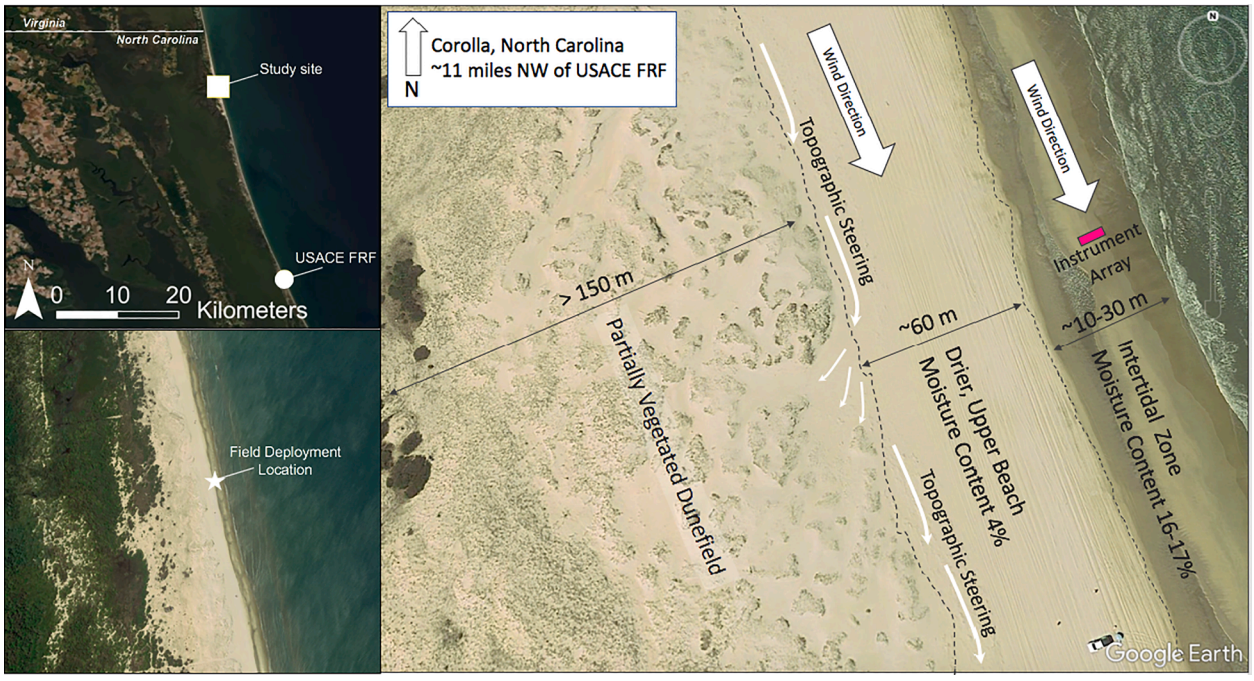


**Fig. 1.** Study Area. Data were collected in the intertidal zone of a dissipative, fine-grained beach north of Corolla, NC, USA. Surface sediment samples were collected on the drier, upper beach and at the instrument array (magenta rectangle). Samples were initially weighed at the USACE FRF.

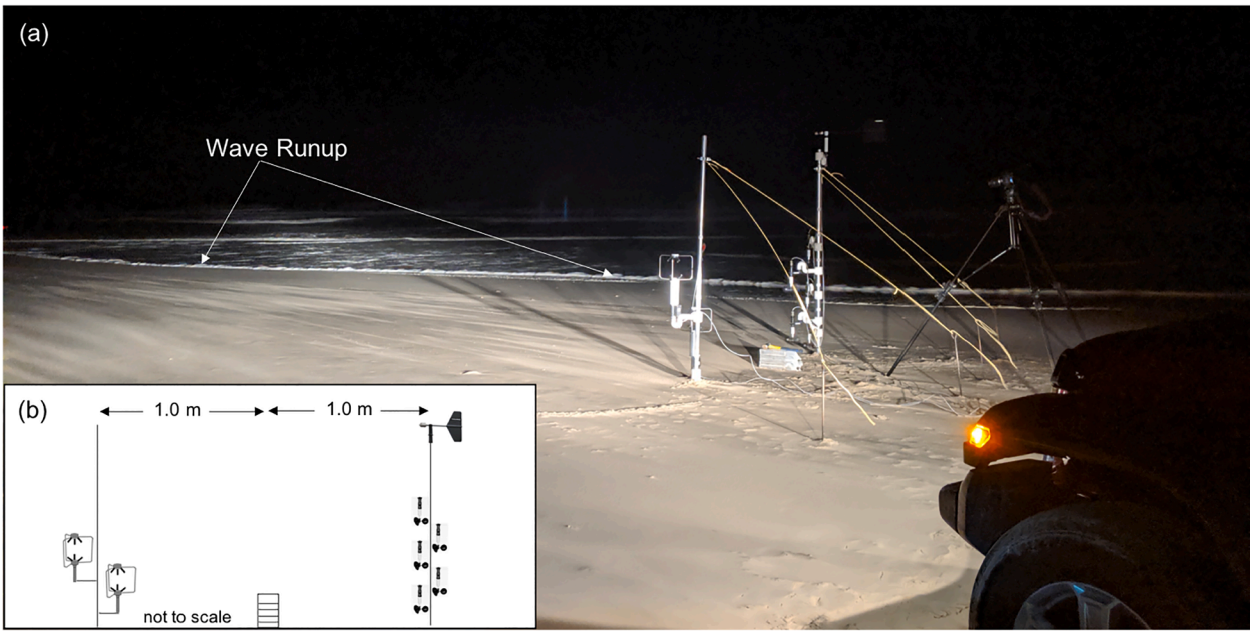


**Fig. 2.** Experimental Setup. Photograph (a) and schematic (b) of the experimental setup during data collection. Data collection occurred during a falling tide on a recently exposed intertidal zone where wave runup varied between 1 and 5 m from the instrument array (b). NNW winds were aligned with the orientation of the shoreline and the instrument array was oriented perpendicular to the dominant wind direction.

A vertical array of saltation traps, developed by Sherman et al. (2014), were used to vertically segregate transport flux, grain size, and moisture content of particles in transport. The elevations of the top of each trap were 0.025, 0.05, 0.075, 0.10 and 0.15 m. All traps had a 0.10 m opening perpendicular to the wind. The four lowest traps had vertical openings of 0.025 m and the highest trap had a vertical opening of 0.05 m (Fig. 2). Saltation trap data were collected over 7, 300 s runs (R1-R7). However, incomplete sediment sampling during R2 prompted its removal from this analysis.

*Moisture content and grain size*

Bed sediments were sampled to a depth of 1 cm at our instrument array at the beginning (0600 h) and end of the experimental runs (0730 h). Bed samples were also taken on the drier, upper beach, pictured in Fig. 1, but only at the beginning of the experiment (~0600 h). Bed and saltation trap sediments were analyzed for bulk gravimetric moisture content and grain size. All sediment samples were sealed immediately upon collection in the field and wet weights of sediments were measured locally at the U.S. Army Engineer Research and Development Center's Field Research Facility within 12 h of collection. Samples were subsequently dried, sieved, and weighed at the NRL Sediment Dynamics Laboratory to determine grain size and gravimetric moisture content. Mean grain sizes were derived using Folk and Ward's Geometric method.

*Transport flux rates and model comparison*

Total flux rates observed during each of our runs, $Q_{total}$, are compared to the models of Bagnold (1936), Kawamura (1951), Zingg (1953), and Lettau and Lettau (1978). Each model has an empirically-derived coefficient, $C$, that calibrates each individual model to predict transport flux using their observed wind tunnel data, Table 1. Sherman et al. (2013) found a substantial reduction in error between predicted and observed transport flux when using recalibrated flux models. We use both the original model coefficients and the field-calibrated model coefficients derived by Sherman et al. (2013) to compare our total flux rates with predicted flux, Table 1.

Shear velocity was determined for each run using the vertical array of cup anemometers. Wind speeds, $u$, were averaged at each height, $z$, over the duration of each run to derive a time-averaged shear velocity. Based on von Kármán's Law of the Wall:

$$u(z) = \frac{u_*}{\kappa} \ln\left(\frac{z}{z_0}\right) \quad (1)$$

where $\kappa$ is equal to 0.4 and $z_0$ is the aerodynamic roughness, we estimate shear velocity, $u_*$, using the slope, $m$, of the log-linear velocity profile:

$$u_* = m\kappa \quad (2)$$

Sherman et al. (2013) and Li et al. (2010) proposed an additional

**Table 1**
Transport flux model coefficients and root-mean squared error.

| Models calculated with Bagnold (1936) threshold shear velocity for dry sediments | | | | | | |
|---|---|---|---|---|---|---|
| Model | Q(C) | RMSE | Q($C_k$) | RMSE | Q($C_{ka}$) | RMSE |
| Bagnold (1936) | 1.80 | 2.96 | 0.79 | 5.95 | 1.41 | 5.38 |
| Kawamura (1951) | 2.78 | 15.86 | 0.70 | 3.79 | 1.27 | 3.81 |
| Zingg (1953) | 0.83 | 4.49 | 0.77 | 4.79 | 1.38 | 4.29 |
| Lettau and Lettau (1971) | 6.70 | 16.04 | 1.20 | 5.12 | 2.47 | 4.47 |
| Models calculated with Belly (1964) threshold shear velocity for moist sediments | | | | | | |
| Model | Q(C) | RMSE | Q($C_k$) | RMSE | Q($C_{ka}$) | RMSE |
| Kawamura (1951) | 2.78 | 39.24 | 0.70 | 15.29 | 1.27 | 23.92 |
| Lettau and Lettau (1971) | 6.70 | 17.77 | 1.20 | 10.28 | 2.47 | 12.71 |

method to estimate shear velocity that scales with the total transport flux, $Q$, to account for changes in the near bed flow velocities due to the retardation of flow by the presence of saltating grains. They predict variability in the von Karman constant, $\kappa$, as a function of $Q$, and estimate shear velocity using the apparent von Karman, $\kappa_a$, constant derived by Li et al. (2010):

$$\kappa_a = -0.003Q + 0.399 \tag{3}$$

which, combined with Eq. (2), can be used to determine a transport flux corrected shear velocity, $u_{*\kappa a}$:

$$u_{*\kappa a} = m\kappa_a \tag{4}$$

We use both methods to predict $Q$ for the field-calibrated transport flux for each model: $Q(C_k)$ denotes the use of Eq. (2) where $\kappa = 0.4$ and $Q(C)_{\kappa a}$ denotes the use of $\kappa_a$ to estimate $u_*$ using Eqs. (3) and (4). Root mean squared errors (RMSE) are calculated for the original and field-calibrated model coefficients to assess model performance.

### *Vertical flux profiles*

It is necessary to normalize vertical flux profiles for comparison between disparate field datasets and for varying trap heights (Ellis et al., 2009). Here, we follow the protocol from Ellis et al. (2009), Li et al. (2009), and Farrell et al. (2012) to resolve normalized vertical, mass flux (g/m/s), $Q_{ni}$ :

$$Q_{ni} = \frac{\frac{Q_i}{h_{ti}-h_{bi}}}{\sum_{i=T_1}^{T_n}(Qi)} \tag{5}$$

Observed transport flux, $Q_i$, at each height is calculated over duration of each run using the total weight of sediment captured in trap, $T_i$. The elevation of the top ($h_{ti}$) and bottom ($h_{bi}$) of each individual trap is used to normalize transport by trap height. We estimate the geometric center of each trap, $GC$, as proposed by Ellis et al. (2009):

$$GC = \sqrt{h_{ti} * h_{bi}} \tag{6}$$

Analogous to Ellis et al. (2009), we find unreasonable estimates of $GC$ at our lowest trap as $h_{bi} = 0$. To resolve this unrepresentative $GC$, we use an estimate of the saltation-enhanced roughness length, $z_0 = 1.0\ mm$. The resulting $GC$ for our lowest trap is $5.0mm$ where $h_{ti} = 25\ mm$ and $h_{bi} = z_0$.

Field observations of aeolian flux profiles are often fit with power or exponential decay functions (Ellis et al., 2009; Li et al., 2009; Farrell et al., 2012; Rotnicka, 2013). Following previous methods for fitting vertical flux profiles over dry beds, we use a least-squares regression to fit $GC$ to $Q_{ni}$ to find $\alpha$ and $\beta$ for both exponential decay (Eq. (7)) and power (Eq. (8)) functions:

$$Q_{ni}(z) = \alpha^{\beta h} \tag{7}$$

$$Q_{ni}(z) = \alpha h^{\beta} \tag{8}$$

where $h$ is the $GC$ height, $\alpha$ and $\beta$ are free fit parameters, and $Q_{ni}$ is the normalized flux value at $h$.

We compare our vertical flux profiles observed over a wet bed with previously published field-derived profiles collected over dry beds. Here, we exclude observations of flux profiles obtained in wind tunnels. We found 3 dry bed datasets and follow the normalization protocols noted above: Ellis et al. (2009), Li et al. (2010) and Farrell et al. (2012). The Ellis et al. (2009) dataset is an aggregation of vertical flux profiles collected over dry, flat sand sheets. Li et al. (2009) collected vertical flux profiles over a dry flat surface near the top of a parabolic dune, and Farrell et al. (2012) profiles were observed over a dry, rippled surface. We refer the readers to each individual publication for more information regarding each dry bed dataset.

Bagnold (1936) delineated between the fluid and impact thresholds via an empirical constant,$A$, derived from his wind tunnel experiments over dry beds. In his formulation, threshold shear velocity, $u_{*_t}$ is scaled by the $A$ parameter:

$$u_{*_t} = A\sqrt{\left(\frac{\rho_s - \rho}{\rho}\right)gd} \tag{9}$$

where $\rho_s - \rho$ are the sediment and fluid densities, $g$ is gravity, and $d$ is the mean grain size. He found $A = 0.1$ for the fluid threshold. Using Bagnold's formulation, Belly (1964) resolved the fluid threshold over a wet surface, $u_{*tw}$, scaled by the percent moisture content ($w$%) of the bed:

$$u_{*_{tw}} = u_{*_t}(1.8 + 0.6\log(w)) \tag{10}$$

## Results and discussion

### *Meteorological and beach surface conditions during data collection*

We successfully collected six runs of total transport flux and vertical flux profiles over a very wet, sandy intertidal zone. Average wind velocities were 9.0 m/s at 93 cm above the surface with gusts reaching 13.5 m/s. Predominate winds were from the NNW and were aligned with beach orientation (NNW-SSE) which provided a constant fetch and sediment supply. No rainfall occurred during data collection, although high humidity was inferred from condensation on field gear. The height of the anemometry increased by 0.5 cm from the beginning and end of experimental runs, ~1.5 h respectively, indicating the surface eroded during the observational period. Surface moisture dropped minimally in the intertidal zone from 17% at 0600 h to 16% at 0730 h. These estimates are likely skewed as the depth of samples were 1 cm and surface grains were likely drier. Moisture content of the upper beach sediments was 2% at 0600 h. Surface sediment samples collected at the instrument array had mean grain size, $\overline{d}$ between 0.17 and 0.19 $mm$. Captured saltating particles had similar grain size distribution to the surface sediments collected at the instrument array, $\overline{d} = 0.16 - 0.18\ mm$. The drier, upper beach sediments were slightly coarser, $\overline{d} = 0.19\ mm$, than the captured saltation in the intertidal zone. Slight differences in grain size distributions were not statistically significant.

Wind speeds, shear velocities, total transport flux, and vertical flux profiles are summarized in Fig. 3. Histograms of measured wind speeds at the lowest (solid bars) and highest (transparent bars) cup anemometers are shown for each Run in Fig. 3a. Fig. 3b shows the time series of instantaneous and 15-second average shear velocities. Shear velocities averaged over the entire run ranged from 0.27 to 0.49 m/s, Fig. 3b. Non-normalized, dry weights of the vertical flux profiles and total flux rates are shown in Fig. 3c. The highest average shear velocity of 0.49 m/s and the highest transport flux of 18.42 g/m/s was observed during Run 4 (Fig. 3c).

### *Threshold shear velocity*

Field-derived shear velocities show that transport can occur below Belly's (1964) fluid threshold. The fluid threshold, $u_{tw}$, for $w\% = 16$ is $0.49m/s$ and greater than the mean shear velocity for all runs (Fig. 3b), except R4 where $u_{*tw} = u_*$. In all cases, the threshold was at least instantaneously exceeded (Fig. 3b). However, the frequency of exceedance is minimal for R5 which corresponded to our smallest observed transport rates ($Q_{total} = 2.47g/m/s$). This suggests that, at the high moisture contents observed, the duration and frequency of these intermittent periods of threshold exceedance have a strong effect on the observed flux.

Our results highlight three main uncertainties that arise in the determination and application the fluid threshold shear velocity to transport occurring over wet beds: (1) the reliance of time-averaging to estimate statistically reliable shear velocities, (2) upwind sediment mobilization, and (3) potential variability in the impact threshold imposed by wet sediments. The fluid threshold shear velocity is a time-

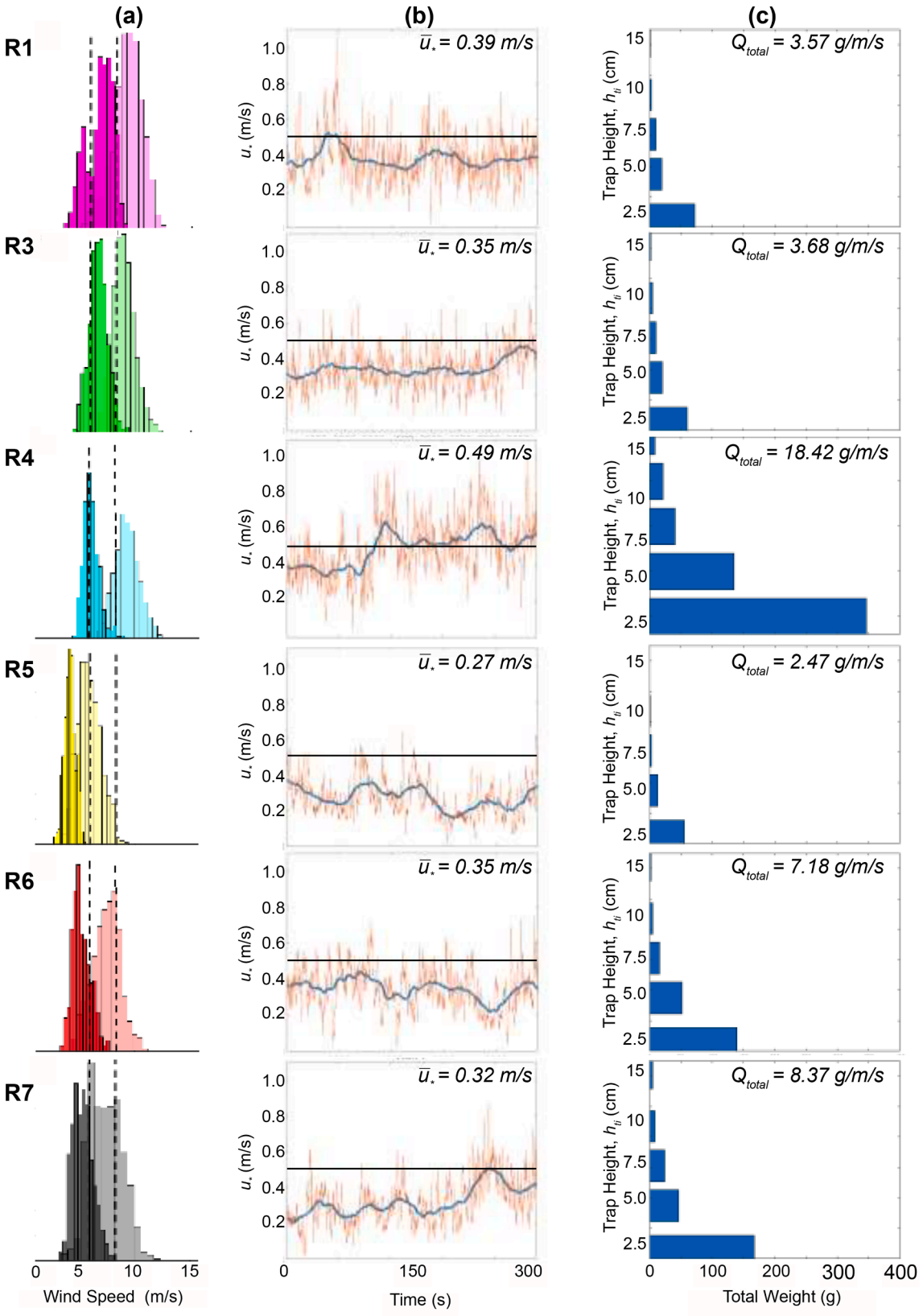


**Fig. 3.** Field Data. Summary diagram of (a) histograms of wind speeds at 7 cm (solid bars) and 93 cm (transparent bars) for each run, (b) instantaneous shear velocity plotted with a 15-second average (blue solid line) and the Belly (1964) fluid threshold (solid horizontal line), and (c) non-normalized vertical flux captured in each trap. Histograms of highest (transparent) and lowest (solid) cup anemometers are shown in (a) to illustrate the gradients in velocity during each run. Mean shear velocity, $\overline{u}_*$, for the entire run is reported along with the total (height-integrated) transport flux, $Q_{total}$ (c).

**Table 2**
Summary of transport data for all runs.

| | | Trap 1 | Trap 2 | Trap 3 | Trap 4 | Trap 5 |
|---|---|---|---|---|---|---|
| Run | Top of Trap (m) | 0.025 | 0.05 | 0.075 | 0.1 | 0.15 |
| | *GC* (m) | 0.005 | 0.035 | 0.061 | 0.087 | 0.122 |
| R1 | *Mass (g)* | 72.50 | 19.81 | 10.14 | 3.29 | 1.40 |
| Duration: 300 s | *Mass (%)* | 67.67 | 18.49 | 9.46 | 3.07 | 1.31 |
| $u_*$ : 0.39 m/s | *Qi* | 2.42 | 0.66 | 0.34 | 0.11 | 0.05 |
| $Q_{total}$: 3.57 g/m/s | *Qni* | 27.07 | 7.40 | 3.79 | 1.23 | 0.26 |
| *d*: 0.17 mm | *w%* | 6.52 | 0.21 | 0.07 | 0.03 | 0.07 |
| | $d_{trap}$ *(mm)* | 0.17 | 0.17 | 0.17 | 0.18 | 0.17 |
| R3 | *Mass (g)* | 60.37 | 21.01 | 10.32 | 5.11 | 2.57 |
| Duration: 270 s | *Mass (%)* | 60.75 | 21.14 | 10.38 | 5.14 | 2.59 |
| $u_*$: 0.35 m/s | *Qi* | 2.24 | 0.78 | 0.38 | 0.19 | 0.10 |
| $Q_{total}$: 3.68 g/m/s | *Qni* | 24.30 | 8.46 | 4.15 | 2.06 | 0.52 |
| *d*: 0.17 mm | *w%* | 1.40 | 0.91 | 0.08 | 0.02 | 0.04 |
| | $d_{trap}$ *(mm)* | 0.17 | 0.17 | 0.17 | 0.17 | 0.18 |
| R4 | *Mass (g)* | 346.42 | 134.69 | 41.25 | 21.64 | 9.03 |
| Duration: 300 s | *Mass (%)* | 62.64 | 24.35 | 7.46 | 3.91 | 1.63 |
| $u_*$: 0.49 m/s | *Qi* | 11.53 | 4.49 | 1.38 | 0.72 | 0.30 |
| $Q_{total}$: 18.42 g/m/s | *Qni* | 25.04 | 9.75 | 2.99 | 1.57 | 0.33 |
| *d*: 0.16 mm | *w%* | 14.99 | 4.45 | 0.00 | 0.21 | 0.04 |
| | $d_{trap}$ *(mm)* | 0.17 | 0.16 | 0.16 | 0.16 | 0.16 |
| R5 | *Mass (g)* | 56.08 | 12.92 | 3.26 | 1.51 | 0.32 |
| Duration: 300 s | *Mass (%)* | 75.69 | 17.44 | 4.40 | 2.04 | 0.43 |
| $u_*$: 0.27 m/s | *Qi* | 1.87 | 0.43 | 0.11 | 0.05 | 0.01 |
| $Q_{total}$: 2.47 g/m/s | *Qni* | 30.28 | 6.98 | 1.76 | 0.82 | 0.09 |
| *d*: 0.16 mm | *w%* | 0.52 | 0.05 | 0.31 | 0.00 | 0.00 |
| | $d_{trap}$ *(mm)* | 0.16 | 0.16 | 0.16 | 0.16 | 0.16 |
| R6 | *Mass (g)* | 139.71 | 52.25 | 16.47 | 4.80 | 2.20 |
| Duration: 300 s | *Mass (%)* | 64.85 | 24.25 | 7.65 | 2.23 | 1.02 |
| $u_*$: 0.35 m/s | *Qi* | 4.66 | 1.74 | 0.55 | 0.16 | 0.07 |
| $Q_{total}$: 7.18 g/m/s | *Qni* | 25.94 | 9.70 | 3.06 | 0.89 | 0.20 |
| *d*: 0.16 mm | *w%* | 4.04 | 0.86 | 0.09 | 0.02 | 0.05 |
| | $d_{trap}$ *(mm)* | 0.17 | 0.16 | 0.16 | 0.16 | 0.16 |
| R7 | *Mass (g)* | 167.09 | 46.58 | 24.06 | 8.73 | 4.68 |
| Duration: 300 s | *Mass (%)* | 66.53 | 18.55 | 9.58 | 3.48 | 1.86 |
| $u_*$: 0.32 m/s | *Qi* | 5.57 | 1.55 | 0.80 | 0.29 | 0.16 |
| $Q_{total}$: 8.37 g/m/s | *Qni* | 25.94 | 9.70 | 3.06 | 0.89 | 0.20 |
| *d*: 0.16 mm | *w%* | 1.28 | 0.96 | 0.68 | 0.00 | 0.04 |
| | $d_{trap}$ *(mm)* | 0.17 | 0.16 | 0.16 | 0.16 | 0.16 |

independent parameter that predicts the minimum shear velocity needed to mobilize sediments in any given environment. Momentary exceedances of the fluid threshold can induce a cascade of transport downwind and transport will continue until the shear velocity falls below the impact threshold necessary to sustain motion. However, several issues arise when predicting the onset and cessation of transport over wet surfaces. First, time-averaging is required to predict statistically reliable estimates of shear velocity using field observations (Bauer et al., 1998; Namikas et al., 2003; Wiggs et al., 2004; Martin et al., 2013). Instantaneous turbulent fluctuations produce deviations from the log-linear velocity profile predicted by Eq. (1). Time-averaging filters these turbulent fluctuations and the correlation between transport and shear velocity systematically improves with increasing averaging intervals (Namikas et al., 2003; Wiggs et al., 2004; Martin et al., 2013). Errors in shear velocity estimates increase for time averaging intervals less than 10 to 15 s (Namikas et al., 2003). Thus, predicting momentary exceedances of the fluid threshold shear velocity is difficult in field environments. In Fig. 3b, we plot instantaneous and 15-second averaged shear velocities for each individual run and also report the mean shear velocity averaged over the length of each run. In almost all cases (except Run 4), transport occurred at time-averaged shear velocities below Belly's (1964) fluid threshold.

While Belly's (1964) fluid threshold is a time-independent parameter, rapid drying of surface sediments makes it difficult to precisely measure moisture content, *w*%, in field environments. Here, we use surface grab samples collected from the surface to a depth of 1 cm to estimate moisture content of surface sediments. The thin layer of material at the surface is likely drier than the grains at 1 cm below the surface, thus our estimates of moisture content are likely skewed. We encourage the development of field techniques capable of remotely measuring moisture content directly at the surface, such as those recently developed by Nield et al. (2011), Smit et al. (2019) and Jin et al. (2020).

An additional uncertainty lies in the determination of the fluid threshold over wet surfaces with a long upwind fetch (10s to 100s of meters). In the present field study, we were unable to measure the upwind spatial variability of moisture content. During our observations, pulses of transport in the form of nested streamers transported particles from upwind through our instrument array and we observed particle mobilization via the impacts of saltating grains. Hence, we believe the fluid threshold was already exceeded at some distance upwind and we simply observed the transport of particles at shear velocities above the impact threshold. However, to date there are no models that predict the impact threshold over wet beds. Subsequent field efforts should account for upwind moisture content and the resulting fetch effects to determine how the fluid impact threshold changes in highly time-varying, moist systems. In order to predict the duration and frequency of transport over wet surfaces, more work is needed to elucidate moisture content of sediments upwind, fetch effects, and the interplay between the fluid and impact thresholds over wet beds.

*Moisture content of sediment in transport*

Our results indicate that particles in transport for all runs were wet. Gravimetric moisture content of sediments captured in each trap are reported in Table 2. The highest moisture contents were consistently found in the lowest trap ($h_{ti} = 0.025$m) with Runs 1, 4 and 6 reaching $w$% of 6.5, 15.0 and 4.0, respectively. Moisture content rapidly decreased with height in all runs (Table 2). Only R5 (the run with the lowest trapped mass) had moisture content less than 1% in the lowest trap. Trapped sediments likely dried to some degree as they were exposed to wind over the duration of each run (300 s or less). In particular, traps above 0.025 m would have been exposed to stronger winds and smaller captured volumes and likely experienced faster drying rates than sediments caught in the lowest trap. Given the inferred high humidity of the field-site and the large timescales of evaporation relative to the sampling time of the field measurements, it is also possible that the upper trap measurements are accurate and that the lower trap measurements are abnormally high. Because of these uncertainties, the moisture contents of the captured samples are likely skewed to some degree.

Particles moving below 0.025 m were particularly wet during Run 4, with the lowest trap $w\% = 15$ nearly equivalent to the $w$% of the bed ($w\% = 16-17$). The wet and dry weights of this sample were 399 g and 346 g. The large mass of the sediment caught in the lowest trap may have reduced the drying time of trapped sediments. The nearly equivalent moisture content suggests that these particles were ejected directly from the surface during this run causing a substantial portion of the measured erosion as R4 corresponded with the highest total fluxes. Thus, the lowest trap may have captured a larger fraction of freshly exposed sediments, i.e. minimal exposure to the wind that could result in drying of sediments.

It is difficult to decipher if the moisture content of the captured particles were (1) simply being ejected from the wet, intertidal zone for all runs, (2) originally drier and acquired moisture as they collided with the surface as they were transported downwind, or (3) a combination of the two scenarios. During our data collection, transport was dominated by long pulses of transport followed by periods of no motion, suggesting that mobilized sediments were from an upwind source. In this scenario, captured wet particles could have mobilized from the drier, upper beach some distance upwind of the study area and acquired moisture as they collided with the more wet bed in the intertidal zone. It is also possible that drier sediments from upwind (sourced from the upper beach or rapid drying of the surface layer on the lower beach) may have carried sufficient momentum to eject more wet particles at rest. These ejected particles could have gained additional momentum from the wind and transitioned to saltation after a series of collisions with the surface. However, the erosion of the surface by 0.5 cm during the observational period suggests that, at least some portion of the time, the particles were ejected directly from the wet bed.

In the extant aeolian literature, particles in transport are assumed to be dry. Here, we observe wet particles moving over a wet bed. The aeolian transport of wet particles has significant implications for the underlying mechanics governing transport. Films of water on saltating particles could increase the weight of individual grains which could alter saltation trajectories and/or impart higher momentum upon collision with the surface. Additionally, wet particles at rest may require more momentum to be ejected from very wet beds due to liquid induced grain-grain cohesion. As we will see in the following sections, vertical flux profiles and transport flux model prediction reflect a difference in the dynamics of transport of wet particles over very wet beds as compared to the transport over dry beds.

*Observed transport flux and vertical flux profiles over wet beds*

Observed total flux, $Q_{total}$, and the distribution of flux with height for each run are summarized in Table 2. Flux rates ranged from 2.47 to 18.42 g/m/s. The highest total transport flux occurred during Run 4, where visual observation during data collection indicated that transport

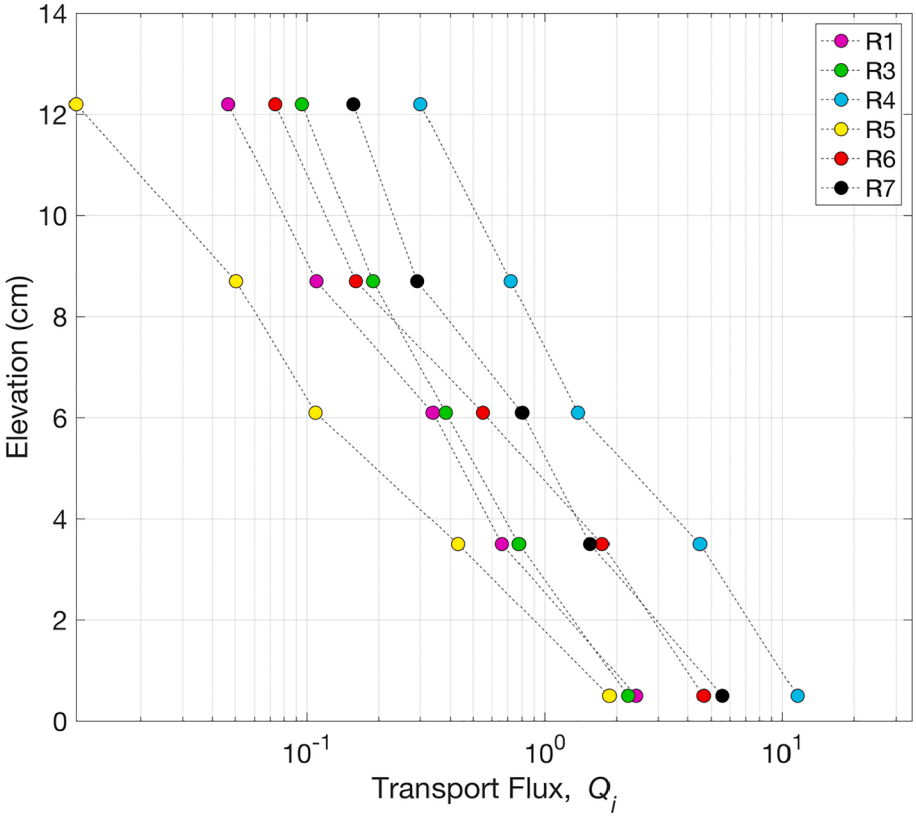


**Fig. 4.** Observed vertical flux profiles over a wet bed. Transport flux, $Q_i$, is plotted with the geometric center, $GC$, of each trap.

**Table 3**
Comparison of transport over dry and wet beds.

| Dataset | *d (mm)* | % of $Q_{total}$ below 0.025 *m* | Exponential fit | | | | Power fit | | | | Site characteristics |
|---|---|---|---|---|---|---|---|---|---|---|---|
| | | | $\alpha$ | $\beta$ | $r^2$ | *RMSE* | $\alpha$ | $\beta$ | $r^2$ | *RMSE* | |
| Ellis et al. (2009) modified: Dry Bed | 0.39 | 32–36 | 12.9 | −0.01 | 0.94 | 0.97 | 21.8 | −0.38 | 0.76 | 2.03 | Flat, sand sheet |
| Farrell et al. (2012): Dry Bed | 0.26–0.35 | 37–52 | 13.9 | −0.02 | 0.96 | 0.89 | 28.3 | −0.46 | 0.85 | 1.78 | Dry rippled surface |
| Li et al. (2009): Dry Bed | 0.27–0.35 | 42–63 | 18.9 | −0.02 | 0.95 | 1.31 | 43.6 | −0.57 | 0.87 | 2.20 | Near top of large parabolic |
| This Study: Wet Bed | 0.17 | 61–75 | 32.1 | −0.04 | 0.99 | 1.11 | 95.4 | −0.80 | 0.96 | 1.96 | In intertidal zone |

was continuous throughout the 300 s run. During all other runs, transport was intermittent and marked with pulses of transport followed by periods of no motion. The distributions of transport flux, $Q_i$, with elevation, *GC*, are shown in Fig. 4. Transport flux in the lowest trap, Trap 1 ($h_{ti} = 0.025$ m) ranged from 1.86 to 11.53 g/m/s. Our flux profiles show a rapid decrease in flux between Trap 1 and Trap 2 ($h_{ti} = 0.05$ m) where transport flux in Trap 2 decreases to 0.43 to 1.74 g/m/s. Despite variability in transport flux, normalized flux profiles are consistent between all runs indicating the distribution of transport with height was consistent for each run.

Between 61% and 75% of the total flux was captured below 0.025 m and up to 82% − 89% of the total flux was captured below 0.05 m. Thus, the percentage of total flux moving close to the surface is much larger than those reported for dry surfaces (Ellis et al., 2009; Li et al., 2009; and Farrell et al., 2012) (Table 3). These observations are consistent with the higher concentrations of flux closer to the bed measured by Rotnicka (2013) and Bauer et al. (2014). In Bauer et al. 2014, 80% (and in some cases up to 95%) of the transport occurred below 125 mm at the crest of a dune and referred to this increase in transport flux very close to the bed as the 'foot' of the flux profile. However, flow acceleration up the slope of the dune or presence of roughness elements may have caused the near-bed deviation in typical flux profiles. Rotnicka (2013) found flux profiles were concentrated below 5 cm over wet beds yet attributes the abnormally high concentration close to the bed to measurement error or a larger portion of the transporting population moving in creep. However, Rotnicka (2013) observed a consistent transition in vertical flux profiles between lower and higher mean wind speeds which suggests the transition is not due to measurement error, but rather a change in the fundamental behavior of transported particles that is dependent on wind speed.

## Comparison of transport over wet versus dry beds

### *Vertical flux profiles*

The measured high concentrations of particles close to our wet bed prompted a comparison to flux profiles measured over dry beds. We compare field observations of wet bed flux profiles with field-derived empirical models of flux profiles measured over dry beds to discern the degree of deviation in the wet flux profiles relative to dry flux profiles. Following protocols used to compare flux profiles over dry beds (Ellis et al., 2009; Li et al., 2009; Farrell et al., 2012), we fit aggregated normalized flux, $Q_{ni}$, at each height, *GC*, to derive estimates of $\alpha$ and $\beta$ for both power (Eq. (5)) and exponential (Eq. (6)) functions. A summary of the grain size, site characteristics, and empirical coefficients are reported in Table 3. For transport over wet beds, the exponential function

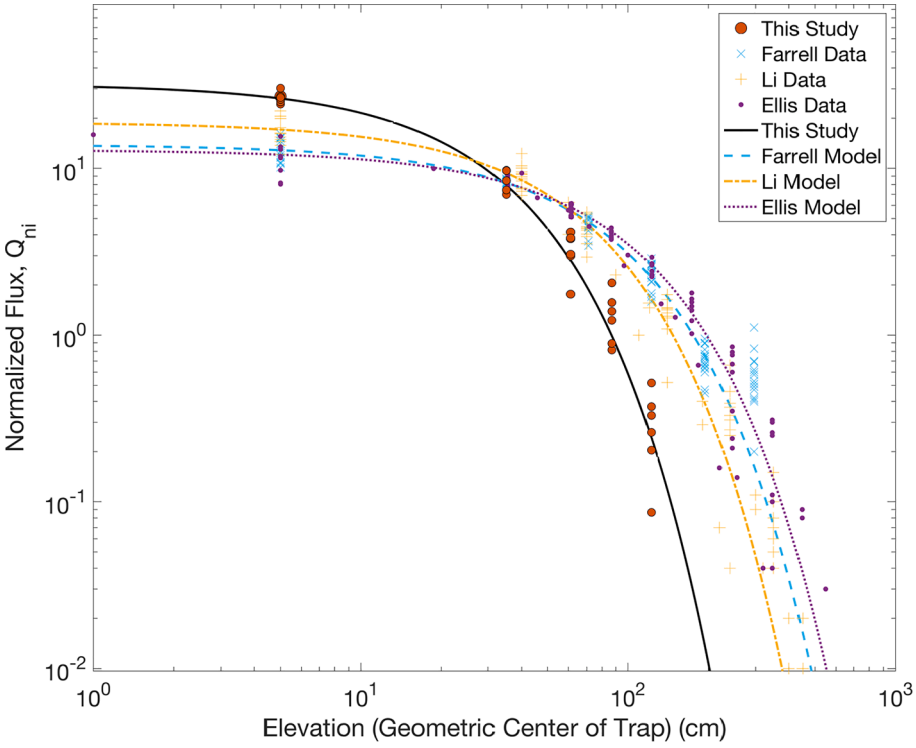


**Fig. 5.** Comparison of normalized vertical flux profiles for wet and dry beds. Experimental data from this study (orange o), Ellis et al. (2009) (purple •), Li et al. (2009) (orange + ), and Farrell et al. (2012) (blue x) are included along with each exponential decay function using $\beta$ and $\alpha$ coefficients reported in Table 3. The distribution of flux with height decreases more rapidly for profiles measured over a wet bed.

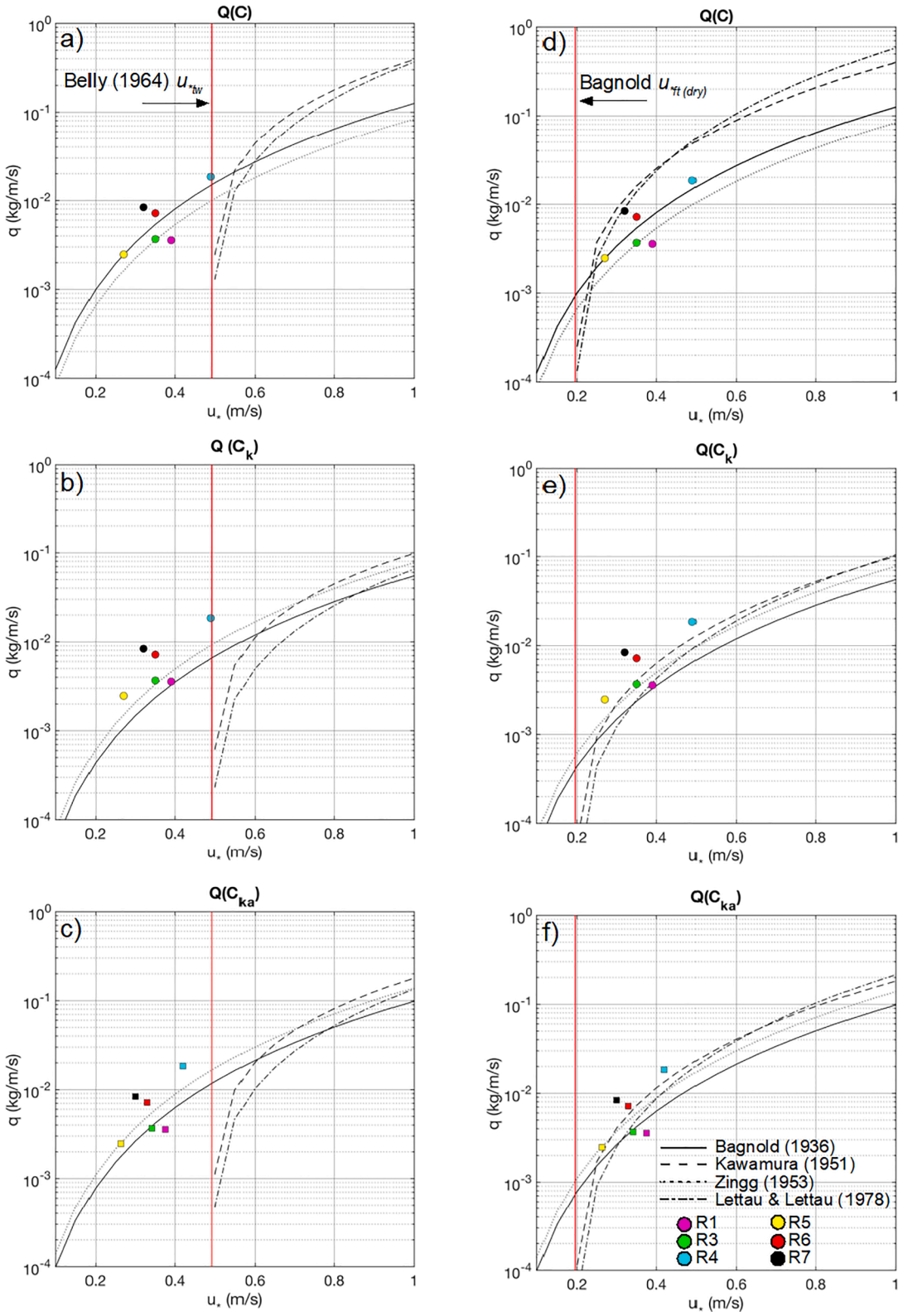


**Fig. 6.** Predicted versus observed flux. Comparison of total flux to predicted flux estimated by the models of Bagnold (1936), Kawamura (1951), Zingg (1953), and Lettau and Lettau (1978) over a wet bed with uncalibrated, $Q_c$, (a,d), field-calibrated, $Q_{ck}$, (b,e) and field-calibrated parameters using the apparent von Karman constant, $Q_{cka}$ (c,f). Mean shear velocity estimated using Eq. (1) for the duration of each run (circles) are shown in 6a, 6b, 6d and 6e, and mean shear velocity estimated using the apparent von Karman constant (Eq. (4)) (squares) are shown in Fig. 6c and f. Models are calculated using Belly's (1964) threshold model (a–c) and Bagnold's (1936) threshold model for dry sediments (d–f). Vertical red line highlights the threshold shear velocity for Belly (1964) and Bagnold (1936). Models estimated with Belly's (1964) threshold (Kawamura (1951) and Lettau and Lettau (1978) produce unrealistic estimates of transport flux and model performance improves when using Bagnold's (1936) threshold shear velocity for dry sediments. Field-calibrated model coefficients derived from Sherman et al. (2013) further reduces error in transport flux models except Bagnold (1936). Root-mean squared error between each model and observed flux are reported in Table 1.

performs slightly better ($r^2 = 0.99$, $RMSE = 1.11$) than the power function ($r^2 = 0.96$, $RMSE = 1.96$) when predicting the vertical flux distribution with height. Using a least-squares regression to resolve the empirical coefficients for the exponential decay function, we find $\alpha$ and $\beta$ to be 32.41 and −0.04. The exponential function also has a better fit to flux profiles measured over dry beds, however, our estimates of $\alpha$ are greater than those found over dry beds (Table 3) indicating more transport occurs closer to the surface for wet beds than that of dry beds. The lower α coefficient in the wet bed case indicates a more rapid decrease in transport flux with height over wet beds, which is reflected in our field observations (Fig. 5).

### *Predicted versus observed flux*

We compared our total flux data, $Q_{total}$, to uncalibrated models of total transport flux, $Q(C)$, and field-calibrated models, $Q(C_k)$ and $Q(C_{ka})$ (Fig. 6). A summary of the model coefficients and their performance is shown in Table 1. We use Belly's (1964) model for threshold shear velocity of wet sediments for the Kawamuara (1951) and Lettau and Lettau (1978) models which require a threshold term. Belly's predicted threshold is high for our wet bed which results in unrealistic model predictions for Kawamura and Lettau and Lettau (Fig. 6a–c). These models predict no or minimal transport as the mean shear velocity does not exceed the threshold of motion except R4 where $u_{*tw} = u_*$. RMSE for uncalibrated and field-calibrated coefficients are greatest for these runs and highlight the inadequacy of using these models when the Belly (1964) threshold is incorporated to predict transport over wet surfaces. While no threshold term is required for the models of Bagnold (1936) or Zingg (1953), the application of these models are based on the conditional statement that $u_* > u_{*t}$. In all observed cases here, $u_* \leq u_{*t}$, thus transport should not occur.

However, we observed substantial transport over our wet bed. This transport could be occurring because the actual value $u_{*tw}$ is lower than the value predicted by Belly's (1964) model which is reasonable given the noted difficulty in determining $u_{*tw}$ (Cornelis and Gabriels, 2003). Another possibility is that the wet bed may have been acting as a transport pathway where sediments moved through the sample volume with minimal exchange between saltation and surfaces sediments. This scenario would negate the use of Belly's (1964) threshold. To test the performance of models in the case that our surface could have acted as a transport pathway, we evaluated Kawamura and Lettau and Lettau using Bagnold's threshold (Eq. (9)) for dry sediments ($u_{*t} = 0.20m/s$). Fig. 6d–f highlights the improvement of Kawamura (1951) and Lettau and Lettau (1978) using Bagnold's dry threshold in predicting transport over wet beds and the corresponding reduction in RMSE is shown in Table 1. RMSE decreases for both uncalibrated and field-calibrated models. The models that do not require a threshold term, the conditional statement $u_* > u_{*t}$ is achieved. The improvement in model performance highlights the need for predicting the threshold of upwind source material and calls into question the use of Belly (1964) to predict transport over wet beds.

The field-calibrated model coefficients, $Q(C_k)$ and $Q(C_{ka})$, generally improve the performance of the tested transport models, with the exception of Bagnold (1936). Our measured total transport flux over a wet bed is best predicted using the original model of Bagnold (1936). Lettau and Lettau (1978) and Kawamura (1951) overpredict flux while Zingg (1953) typically underpredicts transport. The field-calibrated Kawamura (1951), Zingg (1953) and Lettau and Lettau (1978) models show a substantial reduction in RMSE between predicted and observed transport flux (Table 1). $Q(C_{ka})$ estimated with Li et al. (2010)'s apparent von Karman constant (Eq. (3)) further reduces RMSE for Zingg (1953) and Lettau and Lettau (1978). Kawamura (1951) $Q(C_{ka})$ RMSE is nearly equal to the Kawamura $Q(C_k)$ RMSE. As the apparent von Karman constant accounts for the reduction in shear velocity due the concentration of particles, the increased near-bed concentration over wet beds lowers the region of flow retardation. Additionally, we observed pulses of transport, i.e. there were periods without flow retardation due to the presence of saltating particles, and the application of the apparent von Karman constant may only be valid with a continuous time series of transport flux rather than our 300 s bulk observations. The apparent von Karman constant for transport over wet beds should be evaluated in future studies.

One relevant concern is that aeolian transport models are not designed for transport over surfaces with high moisture contents. Over dry beds, the ejection of multiple grains from the impact of single saltating grains results in a rapid increase in total flux (Bagnold, 1936; Andreotti, 2004). However, the presence of water films and wedges increases the adhesion and capillary forces between particles which act to (1) increase bed hardness, and (2) require a stronger force to eject particles at rest (Belly, 1964; Namikas and Sherman, 1995; Comola et al., 2019). These two phenomena can counterbalance total transport rates. Particles impacting hard beds retain more of their momentum as they are transported downwind leading to higher speeds and increased transport flux (McKenna-Neuman and Scott, 1998). However, even with higher impact velocities and higher momentum being imparted onto particles at rest, there is a reduction in the number of ejected particles due to the increase in the force required to mobilize particles at rest. At present, we can find no studies that can tease out these interactions to model the impact threshold required to sustain transport over wet surfaces. An improved estimate of the wet bed impact threshold may provide a more realistic solution than using a dry bed threshold. We believe that the use of an impact threshold for wet beds is needed to adequately predict transport flux in the case where wet beds act as transport pathways.

### *Uncertainty and transport mechanics over wet beds*

Although our field observations cannot tease out the fundamental mechanics governing transport over beds with high moisture contents, we can infer some of the relevant processes. The erosion of the surface by 0.5 cm suggests that, at least for a portion of our observational period, the impact of saltating grains exceeded the force required to eject particles from the bed. High moisture contents of trapped sediments in the lowest traps suggest that ejected particles were likely locally sourced reptation or creep, particularly during Run 4 where trapped sediment in the lowest trap had a moisture content nearly equivalent to the moisture content of the bed. The high concentration of particles close to the bed may have been dominated by a reptating and creep fraction. Alternatively, a decrease in the characteristic rebound height of saltating particles could imply that either (1) ejected grains are not transitioning as effectively into saltation over a wet bed, or (2) beds with moisture content above a certain % do not act as hard surfaces and saltating grains dissipate more energy into the partially wet bed and do not rebound as vigorously.

There is considerable uncertainty in predicting transport over wet beds, specifically in the use of wet-bed threshold models to predict the total transport flux. We find transport can occur well below the fluid threshold for wet beds and highlight the uncertainty associated with Belly's (1964) threshold model, both in the threshold model's conditional application ($u_* > u_{*t}$) for models that do not require a threshold term and model predictions for those that require a threshold term. One source of uncertainty associated with the threshold and resulting flux predictions likely rests with the inability for many models to account for the upwind spatial variability in surface conditions that alter thresholds (e.g. moisture content, grain size). Recently, de Vries et al (2014) developed an advection model to incorporate the upwind spatiotemporal variability of sediment conditions, in particular in supply-limited situations, to better predict flux and surface evolution over time. Models such as these require data of upwind initial conditions, which was absent from the present study, but the authors encourage the use of these types of models. Incorporating the spatial variability of upwind

moisture content and grain size, for example, could reduce error in flux predictions.

We also find the near-bed concentrations of saltating particles to be higher than those observed over dry surfaces. More research is needed to uncover (1) the fundamental mechanisms regulating the observed lower average transport heights over wet beds, (2) the best way to incorporate moisture dependent threshold models, and (3) the validity of models predicting transport flux over wet surfaces.

## Conclusions

In this study, we conducted a field experiment where we observed aeolian transport over a wet, sandy beach. We present measurements of total transport flux, the distribution of flux with height, and the moisture content of particles in transport. We compare our field observations to field-derived empirical models of vertical flux profiles over dry beds and derive our own empirical estimates of flux profiles measured over a wet bed using exponential decay and power functions. Differences in the vertical flux profiles between wet and dry beds indicate that the mechanisms driving transport over wet beds are fundamentally different. More research is needed to tease out the mechanics driving the deviation in flux profiles and the transport of wet sediments. We also find that transport occurs below the threshold of motion predicted by Belly (1964). This indicates that the appropriate $u_{*t}$ necessary to satisfy the conditional application, $u_* > u_{*t}$, for models that do not require a threshold term differs from the $u_{*tw}$ predicted by Belly (1964). Models that require an explicit threshold term also predict transport that deviates from field observations when using the Belly (1964) model. However, errors are generally reduced when applying the threshold for dry sediments and using field-calibrated model coefficients.

From this analysis, we can determine four key conclusions:

- Substantial transport can occur below Belly's (1964) fluid threshold for wet sediments.
- Sediments in transport can be wet and sediments travelling closer to the bed have higher moisture contents.
- At the high transport rates measured, vertical flux profiles over wet beds can exhibit a high concentration of particles very close to the bed with fewer grains reaching the typical saltation heights measured over dry beds. An exponential function fits the wet and dry bed vertical flux distributions.
- Transport flux models predict transport below the fluid threshold of motion for wet beds. Model performance improves when using thresholds for dry sediments indicating that the appropriate threshold lies below that predicted by Belly's (1964) threshold of motion. Another possibility is that wet beds act as passive transport pathways for sediments, though this is confounded by the local bed exchange implied by the observed 0.5 cm of erosion. More work is needed to adequately predict transport flux over wet beds.

Our results and analysis present new field data of sediment transport over wet beds and complement previous studies aimed at discerning total flux and the distribution of flux with height. We highlight the deviation in vertical flux profiles over wet beds when compared to the profiles observed over dry beds. We call for more field observations of transport flux over wet beds over a range of moisture contents and fetch lengths to discern the complex physical interactions of aeolian transport in coastal environments that are often characterized by strong cross-shore moisture gradients.

## Declaration of Competing Interest

The authors declare that they have no known competing financial interests or personal relationships that could have appeared to influence the work reported in this paper.

## Acknowledgements

Christy Swann and Charles Key were supported under base funding to the U.S. Naval Research Laboratory from the Office of Naval Research. Dylan Lee and Sarah Trimble were supported as postdoctoral fellows through the National Research Council Research Associateship Program at the U.S. Naval Research Laboratory. The authors would like to thank Edward Braithwaite, Shawn Harrison, Kara Koetje, and Ryan Philip for their support in preparation for the experiments and Samuel Griffith for processing sediment samples. These data were collected as part of the During Nearshore Event Experiment (DUNEX), which was facilitated by the U.S. Coastal Research Program (USCRP). We also thank the U.S. Army Engineer Research and Development Center's Field Research Facility for the use of their facility and support of their operations staff.

## References

Andreotti, B., 2004. A two-species model of aeolian sand transport. J. Fluid Mech. 510, 47–70.
Bagnold, R.A., 1936. The movement of desert sand, Proceedings of the Royal Society of London. Series A, Mathematical and Physical Sciences, 257(892): 594-620.
Barnocky, G., Davis, R.H., 1989. The lubrication force between spherical drops, bubbles and rigid particles in a viscous fluid. Int. J. Multiph. Flow 15 (4), 627–638.
Bauer, B.O., Yi, J., Namikas, S.L., Sherman, D.J., 1998. Event detection and conditional averaging in unsteady aeolian systems. J. Arid Environ. 39, 345–375.
Belly, P.Y., 1964. Sand movement by wind. Monograph, Hydraulic Engineering Laboratory, Wave Research Physics, University of California, Berkeley, CA.
Chepil, W.S., 1945. Dynamics of wind erosion: II Initiation of soil movement. Soil Sci. 60 (5), 397.
Comola, F., Gaume, J., Kok, J.F., Lehning, M., 2019. Cohesion-induced enhancement of aeolian saltation. Geophys. Res. Lett. 46, 5566–5574.
Cornelis, W.M., Gabriels, D., 2003. A simple model for the prediction of the deflation threshold shear velocity of dry loose particles. Sedimentology 51, 39–51.
Davidson-Arnott, R.G.D., Bauer, B.O., Hesp, P.A., Namikas, S., Ollerhead, J.W., Walker, I. J., 2005. Moisture and fetch effects on aeolian sediment transport rates during a Fall storm, Greenwich dunes, Prince Edward Island. In Proceeding, Canadian Coastal Conference, Halifax. National Research Council, Ottawa, 2005.
Davidson-Arnott, R.G.D., Bauer, B.O., 2009. Aeolian sediment transport on a beach: Thresholds, intermittency, and high frequency variability. Geomorphology 105, 117–126.
Davis, R.H., Rager, D.A., Good, B.T., 2002. Elastohydrodynamic rebound of spheres from coated surfaces. J. Fluid Mech. 468, 107.
de Vries, S., Arens, S.M., de Schipper, M.A., Ranasinghe, R., 2014. Aeolian sediment transport on a beach with a varying sediment supply. Aeolian Res. 14, 235–244.
Delgado-Fernandez, I., Davidson-Arnott, R.G.D., 2011. Meso-scale aeolian sediment input to coastal dunes: The nature of aeolian transport events. Geomorphology 126, 217–232.
Ellis, J.T., Li, B., Farrell, E.J., Sherman, D.J., 2009. Protocols for characterizing aeolian mass-flux profiles. Aeolian Res. 1, 19–26.
Farrell, E.J., Sherman, D.J., Ellis, J.T., Li, B., 2012. Vertical distribution of grain size for wind blown sand. Aeolian Res. 7, 51–61.
Han, Q., Qu, J., Liao, K., Zhang, K., Zu, R., Niu, Q., 2012. A wind tunnel study of the parameters for aeolian sand transport above a wetted sand surface using sand from a tropical humid coastal region of southern China. Environ. Earth Sci. 67, 243–250.
Horikawa, K., Hotta, S., Kraus, N.C., 1986. Literature review of sand transport by wind on a dry sand surface. Coast. Eng. 9, 503–526.
Hotta, S., Kubota, S., Katori, S., Horikawa, K., 1984. Sand transport by wind on a wet sand surface, Proceedings of the 19th Coastal Engineering Conference, 1984, pp. 1265-1281.
Jin, J., de Sloover, L., Verbeurgt, J., Stal, C., Deruyter, G., Montreuil, A., de Maeyer, P., de Wulf, A., 2020. Measuring surface moisture on a sandy beach based on corrected intensity data of a mobile terrestrial lidar. Remote Sens. 12 (2) https://doi.org/10.3390/rs12020209.
Kawamura, R., 1951. Study on sand movement by wind. Reports of Physical Sciences Research Institute of Tokyo University, 5: 95-112 [translated from Japanese by National Aeronautics and Space Administration (NASA), Washington D.C., 1972].
Kawata, S., 1950. Field investigation of blown sand on beaches. Forestry Conservation Rep, (2).
Lettau, K., Lettau, H.H., 1978. 'Experimental and micrometeorological field studies of dune migration', In: Lettau, H. and Lettau, K. (Eds), Exploring the World's Driest Climate. University of Wisconsin-Madison IES Report, 101: 110-147.
Li, B., Granja, H.M., Farrell, E.J., Ellis, J.T., Sherman, D.J., 2009. Aeolian saltation at Esposende Beach Portugal. J. Coastal Res., SI 56, 327–331.
Li, B., Sherman, D.J., Farrell, E.J., Ellis, J.T., 2010. Variability of the apparent von Karman parameter during aeolian saltation. Geophys. Res. Lett. 37, L15404.
Martin, R.L., Barchyn, T.E., Hugenholtz, C.H., Jerolmack, D.J., 2013. Timescale dependence of aeolian sand flux observations under atmospheric turbulence. J. Geophys. Res.: Atmos. 118 (16) https://doi.org/10.1002/jgrd.50687.
McKenna-Neuman, C., Scott, M.M., 1998. A wind tunnel study of the influence of pore water on aeolian sediment transport. J. Arid Environ. 39, 403–419.

Namikas, S.L., Sherman, D.J., 1995. A review of the effects of surface moisture content on aeolian sand transport. In: Tchakerian, V.P. (Ed.), Desert Aeolian Processes. Springer, Dordrecht.
Namikas, S.L., Bauer, B.O., Sherman, D.J., 2003. Influence of averaging interval on shear velocity estimates for aeolian transport modeling. Geomorphology 53, 235–246.
Nield, J.M., Wiggs, G.F.S., 2011. The application of terrestrial laser scanning to aeolian saltation cloud measurements and its response to changing surface moisture. Earth Surf. Proc. Land. 36, 273–278.
Nield, J., Wiggs, G.F.S., Squirrell, R., 2011. Aeolian sand strip mobility and protodune development on a drying beach: examining surface moisture and surface roughness patterns measured by terrestrial laser scanning. Earth Surf. Proc. Land. 36 (4), 513–522.
Pitois, O., Moucheront, P., Chateau, X., 2000. Liquid bridge between two moving spheres: An experimental study of viscosity effects. J. Colloid Interface Sci. 231 (1), 26–31.
Rotnicka, J., 2013. Aeolian vertical mass flux profiles above dry and moist sandy beach surfaces. Geomorphology 187, 27–37.
Sherman, D.J., Jackson, D.W.T., Namikas, S.L., Wang, J., 1998. Wind-blown sand on beaches: An evaluation of models. Geomorphology 22, 113–133.
Sherman, D.J., Li, B., Ellis, J.T., Farrell, E.J., Parente Maia, L., Granja, H., 2013. Recalibrating aeolian sand transport models. Earth Surf. Proc. Land. 38, 169–178.
Sherman, D.J., Swann, C., Baron, J., 2014. A high-efficiency, low-cost aeolian sand trap. Aeolian Res. 13, 31–34.
Smit, Y., Donker, J.J.A., Ruessink, G., 2019. Spatiotemporal surface moisture variations on a barred beach and their relationship with groundwater fluctuations. Hydrology 6 (1). https://doi.org/10.3390/hydrology6010008.
van Dijk, P.M., Stroosnijder, L., 1996. The influence of rainfall on transport of beach sand by wind. Earth Surf. Proc. Land. 21, 341–352.
van Rijn, L.C., Strypsteen, G., 2020. A fully predictive model for aeolian sand transport. Coast. Eng. 156, 103600.
Wiggs, G.F.S., Baird, A.J., Atherton, R.J., 2004. The dynamic effects of moisture on the entrainment and transport of sand by wind. Geomorphology 59, 13–30.
Zingg, A.W., 1953. Wind tunnel studies of the movement of sedimentary material. In: Institute of Hydraulics. Iowa City, IA, pp. 111–135.

## *Further reading*

Bauer, B., Davidson-Arnott, R.G.D., 2014. Aeolian particle flux profiles and transport unsteadiness. J. Geophys. Res. Earth Surf. 119, 1542–1563.